Size Effect in the Measurement of Microwave Permeability of Ferrites*

In the usual method of measuring the tensor permeability of ferrites at microwave frequencies, a small sample of the material is placed in a suitable cavity, and the change in resonant frequency and Q of the cavity, caused by the presence of the ferrite, are measured. The measured quantities are related to the quantities of interest—real and imaginary parts of permeability—by equations derived through perturbation theory.[1]

In the derivation of these equations, certain assumptions are made about the effect of insertion of the sample in electromagnetic fields of the cavity. A simple way of stating it is to assume that the fields of the cavity are unchanged, except in the volume occupied by the sample, though there are less restrictive formulations. Therefore, the fields inside of the sample are uniform and thus may be calculated as a static problem from the unperturbated fields in the cavity. Both of these assumptions are approximations, and are more accurate as the sample size decreases.

Although the effect of the finite sample size has been calculated by several investigators, the resulting formulas do not readily lend themselves to computations. As a practical problem, in the comparison of a number of ferrite materials, it is of interest to know how large a sample could be used to obtain the measurements, yet apply the simple perturbation assumptions with confidence. That is, the perturbation formulas are valid for a sample which is sufficiently small. How small is small?

In an attempt to provide a partial answer to this problem, measurements were made on spheres of two typical polycrystalline ferrite R-1, a magnesium manganese ferrite and yttrium iron garnet. The measurements were made by mounting the sample in the center of an X-band TE_{102} rectangular cavity; and the change in the insertion loss as a function of the applied magnetic field was measured. The quantity obtained is u'', the imaginary part of the diagonal element of the permeability tensor. The values of u'' were calculated from the equation

$$u'' = \left(\frac{V_0}{V} - 1\right)\frac{V_c}{4Q_uV_s\left[1 - \left(\frac{\lambda_0}{2_a}\right)^2\right]}.$$

where V_0/V_1 is determined from the ratio of the insertion loss of the cavity at very large static field to the insertion loss at a particular field; Q_u is the unloaded Q of the cavity; V_c and V_s are volume of the cavity and the sample, respectively. This formula gave values of u''_{max} and line width which were independent of size, within experimental uncertainty, for all the samples.

It appears that the largest sizes considered were "small" within the context of perturbation theory. The size of the samples were limited by the sensitivity of the apparatus, *i.e.*, by the largest insertion loss that could be measured using the apparatus shown in Fig. 1. The measured line width and u''_{max} as a function of sample size are shown in Figs. 2 and 3 for R-1 and YIG, respectively. The largest sizes measured were 0.035 inch in diameter for YIG, and 0.069 inch in diameter for R-1. These samples were ground to smaller sizes, so that all the measurements could be made on the same sample of ferrite.

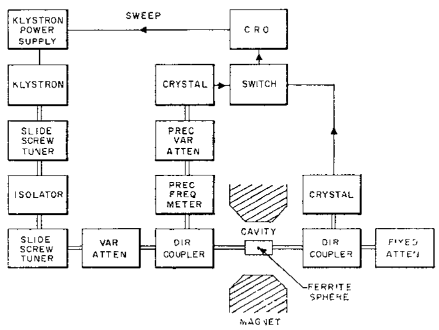

Fig. 1—Block diagram of the apparatus.

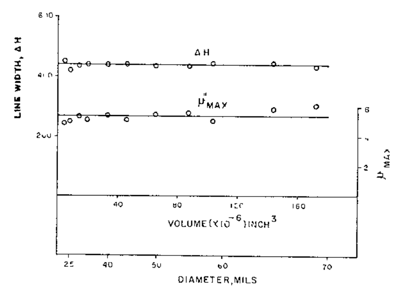

Fig. 2—Line width and u''_{max} as a function of size for R-1 ferrite.

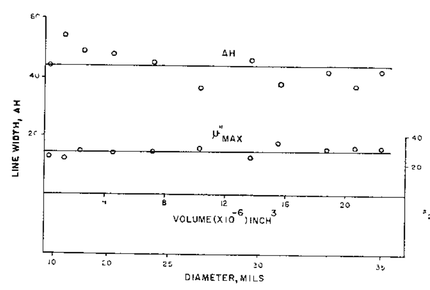

Fig. 3—Line width and u''_{max} as a function of size for YIG ferrite.

The scatter in the measurements was partly due to the change in Q of the cavity, as it was disassembled and reassembled whenever a different size sample was placed in the cavity, and partly due to fluctuations in the static field. The latter was particularly serious for the measurements made on YIG samples.

This paper extends the measurements to larger size samples, in order to compare the experimental results with the calculated values of size effect. The experimental results obtained thus far indicate that the measured values of line width and permeability are independent of size for samples of appreciable volume. These results can be compared to those of Spencer, *et al.*, on R-1[2] and of Stinson on YIG.[3] Stinson's measurements, however, were made by a different technique.

B. Maher
FXR, Inc.
Woodside, N. Y.
L. Silber
Microwave Res. Institute
Brooklyn, N. Y.

* Received by the PGMTT, September 15, 1960. This paper is based on Maher's thesis submitted to the Polytechnic Institute of Brooklyn, Brooklyn, N. Y., in partial fullfilment of the requirements for the M.E.E. degree. The work on which this paper is based was done while the author was a member of the staff of the Microwave Research Institute of the Polytechnic Institute of Brooklyn, and was supported by the Joint Services Technical Advisory Committee under contract AF-18(600)-1505.

[1] J. O. Artman and P. E. Tannenwald, "Measurement of susceptibility tensor in ferrites," *J. Appl. Phys.*, vol. 26, pp. 1124–1132; September, 1955.

[2] E. G. Spencer, R. C. LeCraw, and L. A. Ault, "Notes on cavity perturbation theory," *J. Appl. Phys.*, vol. 23, pp. 130–132; January, 1957.

[3] D. C. Stinson, "Experimental techniques in measuring ferrite line widths with a crossguide coupler," 1958 WESCON Convention Record, pt. 1, pp. 147–150.

Cutoff Variable Reactor*

When relatively high positive reactance is required for coaxial line circuits, the cutoff variable reactor can economize space. In Fig. 1, a schematic diagram of the cutoff variable reactor is shown. For $z<0$, there is the coaxial line; and for $z>0$, there is the cylindrical waveguide operated in cutoff region with the variable shorting plunger shorting the waveguide at the distance s. For simplicity, it is assumed that there is TEM mode alone on the coaxial line and TM_{01} mode alone in the waveguide. The wave equation of H can be solved under these assumptions, together with the following boundary conditions:

$$\left[\frac{\partial H_\phi}{\partial z}\right]_{z=s} = 0 \qquad (1)$$

and the input current,

$$I = \oint_{c_1} [H_\phi]_{z=0}\rho d\phi = -\oint_{c_2} [H_\phi]_{z=0}\rho d\phi. \qquad (2)$$

The integral contours C_1 and C_2 are shown in Fig. 2. The solution is

$$H_\phi = A\{I_1(\sigma\rho) + BK_1(\sigma\rho)\} \cdot \sin\left\{\frac{\pi}{4}\left(\frac{z}{s} + 1\right)\right\}, \qquad (3)$$

* Received by the PGMTT, September 20, 1960.

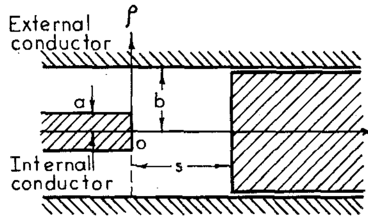

Fig. 1—Cutoff variable reactor.

where both A and B are integrating constants and both I_1 and K_1 are modified Bessel functions.

$$\sigma \equiv \sqrt{\left(\frac{\pi}{4s}\right)^2 - \left(\frac{2\pi}{\lambda}\right)^2} \tag{4}$$

and

$$B = \frac{bI_1(\sigma b) - aI_1(\sigma a)}{aK_1(\sigma a) - bK_1(\sigma b)}. \tag{5}$$

The input voltage is given by

$$V = \int_a^b \left[-\frac{1}{j\omega\epsilon} \frac{\partial H_\phi}{\partial z} \right] d\rho. \tag{6}$$

The input reactance is given by dividing (6) by (2) providing (3),

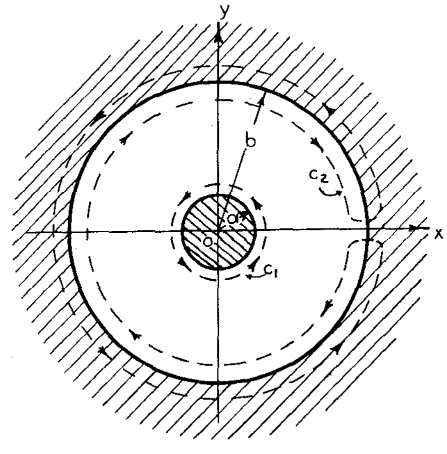

Fig. 2—Integral contour to obtain the input currents.

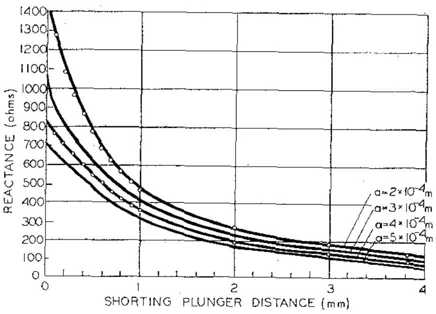

Fig. 3—Reactance of cutoff variable reactor.

$$X_S = \frac{\sqrt{\frac{\mu}{\epsilon}}}{\frac{16\pi}{\lambda} ab\sigma s} \cdot \frac{\{I_0(\sigma b) - I_0(\sigma a)\}\{aK_1(\sigma a) - bK_1(\sigma b)\} - \{K_0(\sigma b) - K_0(\sigma a)\}\{bI_1(\sigma b) - aI_1(\sigma a)\}}{I_1(\sigma b)K_1(\sigma a) - I_1(\sigma_a)K_1(\sigma b)}. \tag{7}$$

For example with $b = 2.25$ mm and $\lambda = 3.07$ cm, the reactance X_s changed as shown in Fig. 3 for various center conductor radii a and shorting plunger distances s. This reactor shows high reactance for small values of shorting plunger distances. When the inner conductor radius is 0.4 mm, in order to have 350 ohms, the conventional coaxial plunger requires a shorting plunger distance of 6.72 mm. On the other hand, the same reactance can be obtained by the cutoff reactor with a shorting plunger distance of 1 mm. This space economization is more effective for higher reactances. For 835 ohms, the shorting plunger distance of the conventional coaxial shorting plunger is 7.25 mm. For the same reactance, the shorting plunger distance of the cutoff reactor is 0.045 mm. The latter case was tested by experiment in a reflex klystron amplifier[1,2] circuit. The results of the experiment agreed with the calculations.

The author extends his thanks to R. Robinson, for numerical computation by IBM 650, and S. Krupnik and J. Stefancin for preparation of the manuscript.

KORYU ISHII
Dept. of Elec. Engrg.
Marquette University
Milwaukee, Wis.

[1] K. Ishii, "X-band receiving amplifier," *Electronics*, vol. 28, p. 202; April, 1955.
[2] K. Ishii, "Amplification circuit for the internal cavity-type reflex klystron," *J. Res. Inst. Tech., Nihon University* (Tokyo, Japan), vol. 14, pp. 1–10; December, 1957.

Single-Mode Cavity Maser at 2200 Mc*

Cavity masers which have been reported in the literature have utilized a dual-mode cavity resonant at the pump and signal frequencies, but Strandberg, *et al.*,[1] has reported an X-band cavity maser which can be operated with the cavity resonant only at the signal frequency. Siegmann[2] has also reported a multiplicity of resonances in his cavity maser for the pump signal which might possibly be caused by some sort of dielectric loading effect.

Both these facts suggested to us that an S-band cavity maser using only a single resonant mode at the signal frequency could be developed by using the ruby itself as the pump circuit. If this scheme were practical, design of tunable cavity masers at S-band would be much simpler than it is. With this thought in mind, a maser cavity circuit suitable for operation from 2100–2500 Mc was designed.

The maser's active material was pink ruby, $Al_2O_3Cr^{+++}$ oriented at an angle $\theta \cong 90°$. The cavity is a re-entrant $\lambda/4$-TEM stripline type in X-band waveguide with loop coupling as depicted in Fig. 1. The resonant frequency of the cavity is determined primarily by the length of center strip and by the ruby volume. The degree of coupling by the loop remained essentially constant over a 400-Mc frequency range. For the cavity filled on both sides as shown in Fig. 1, we estimated the filling factor to be approximately 75 per cent or greater. X-band pump energy is fed directly down the waveguide to the ruby crystals.

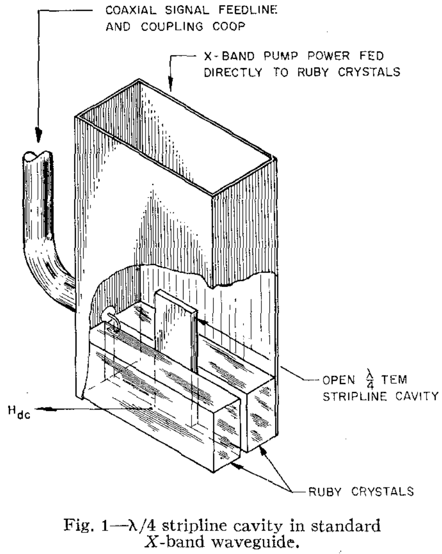

Fig. 1—$\lambda/4$ stripline cavity in standard X-band waveguide.

This cavity maser has been operated from 2120 to 2500 Mc by adjusting the length of the center strip and varying the pump frequency and dc magnetic field. Complete inversion of energy levels was obtained for all frequencies without the use of a pump cavity mode, and no pump resonances of any type were observed.

For the master amplifier characteristics considered here, the resonant frequency was 2200 Mc and the pump frequency was 12,470 Mc. Fig. 2 relates the gain-bandwidth products to the level of input power. This

* Received by the PGMTT, September 20, 1960.
[1] R. J. Morris, R. L. Kuhl, and M. W. P. Strandberg, "A tunable maser amplifier with large bandwidth," PROC. IRE, vol. 47, pp. 80–81; January, 1959.
[2] W. S. C. Chang, J. Cromack, and A. E. Siegman, "Experiments on a High-Performance Cavity Maser Using Ruby at S Band," Electron Devices Lab., Stanford Electronics Lab., Stanford University, Stanford, Calif., Rept. No. T.F. 156-4; July 21, 1959.